

## ACT LAUNCH Project No 299662



The LAUNCH project is funded through the ACT programme (Accelerating CCS Technologies, Horizon2020 Project No 294766). Financial contributions are made from: Netherlands Enterprise Agency (RVO), Netherlands; Bundesministerium für Wirtschaft und Energie (BMWi), Germany; Gassnova SF (GN), Norway; Department for Business, Energy & Industrial Strategy (BEIS) together with extra funding from NERC and EPSRC research councils, United Kingdom; US-Department of Energy (US-DOE), USA.  
All funders are gratefully acknowledged.



Supported by:  
Federal Ministry  
for Economic Affairs  
and Energy  
on the basis of a decision  
by the German Bundestag



Department for  
Business, Energy  
& Industrial Strategy



**Lowering Absorption process UNcertainty, risks  
and Costs by predicting and controlling amine  
degradation**

### **Deliverable Nr. D1.3.4**

**Application: Degradation Network Model: a tool for predicting  
solvent degradation in industrial CO<sub>2</sub> capture applications**

<b>Dissemination level</b>	Public	
Written By	Juliana Monteiro, Melvin Kruijne, Tanya Srivastava (TNO),	Date: 03.02.2023
Checked by WP1 Leader	Andreas Grimstvedt (SINTEF)	Date: 06.02.2023
Approved by the coordinator	Peter van Os (TNO)	Date: 09.02.2023
Issue date	09.02.2023	





## Executive summary

In this deliverable, the Degradation Network Model (DNM) is presented. The model can be applied to any solvent, as it relies solely on oxygen consumption data. The oxygen consumption data used in the current version of the DNM is generated with fresh solvent, in the absence of metals and degradation products. In order to obtain representative values, the stoichiometric factor is treated as a fitting parameter, and used to anchor the DNM results to those observed in the RWE pilot. The DNM methodology is thoroughly discussed in the current deliverable, and the model can be used to predict solvent losses for MEA and CESAR1 at different operational conditions. To improve the model prediction, more data is needed, as extensively discussed throughout this report.

Despite the DNM current limitations, general conclusions can already be taken. For MEA, it is likely that most of the solvent loss occurs already in the absorber packing (low loading, high temperature range). The absorber design could be modified in order to minimize losses – however, it should be taken into consideration that any changes would also affect the CO<sub>2</sub> absorption kinetics. So, any proposed modification should be evaluated with a holistic view, considering CAPEX and OPEX impacts.

For CESAR1, most of the solvent degradation is expected to happen in the absorber sump. Lowering the residence time in the sump wouldn't necessarily lower the degradation but is likely to just push it to the downstream unit operations. A possible solution would be to remove dissolved oxygen from the solvent before it enters the sump. Within LAUNCH, it was demonstrated that DORA is capable of removing at least 90% of DO from CESAR1 (see D2.1.2). Applying the DNM, it is estimated that DORA would lead to a reduction of ca. 80% in the CESAR1 loss (from 150 to 30 g/tonCO<sub>2</sub>).

## Table of Contents

<b>1</b>	<b>INTRODUCTION</b>	<b>5</b>
<b>2</b>	<b>THE DNM DESCRIPTION</b>	<b>6</b>
2.1	COMPARISON WITH OTHER MODELS AVAILABLE IN LITERATURE	7
2.1.1	<i>Léonard et al., 2014</i>	7
2.1.2	<i>Pinto et al., 2014</i>	8
<b>3</b>	<b>LAB SCALE DEGRADATION DATA: ODIN EXPERIMENTS</b>	<b>9</b>
3.1	ODIN DESCRIPTION	9
3.1.1	<i>Chemicals</i>	9
3.1.2	<i>Experimental method</i>	10
3.2	ODIN RESULTS FOR MEA AND DISCUSSIONS	10
3.3	RESULTS FOR CESAR1	14
3.4	DERIVING ORDER OF REACTIONS AND KINETIC PARAMETERS	17
3.4.1	<i>Order of reaction – MEA and CESAR1</i>	17
3.4.2	<i>Kinetics parameters – MEA</i>	20
3.4.3	<i>Kinetics parameters – CESAR1</i>	21
3.5	DNM LIMITATIONS	23
<b>4</b>	<b>DNM APPLICATION</b>	<b>24</b>
4.1	BASE CASE: THE ALIGN-CCUS WTE CASE	24
4.2	DNM APPLIED TO MEA AND CESAR1 WTE CAPTURE PLANTS	24
4.2.1	<i>Setting the stoichiometric factor: RWE data</i>	24
4.2.2	<i>Absorber packing – MEA</i>	25
4.2.3	<i>Absorber packing – CESAR1</i>	26
4.2.4	<i>Absorber sump – MEA and CESAR1</i>	27
4.2.5	<i>Cross heat exchanger – MEA and CESAR1</i>	27
4.2.6	<i>Consolidated results – MEA and CESAR1</i>	28
<b>5</b>	<b>CONCLUSIONS AND FUTURE WORK</b>	<b>30</b>
<b>6</b>	<b>REFERENCES</b>	<b>31</b>

## 1 Introduction

Amine-based post combustion CO<sub>2</sub> capture (PCCC) is a mature technology, demonstrated at full scale, and currently entering implementation phase at various industries. PCCC plants can capture CO<sub>2</sub> from point sources such as power plants, waste-to-energy facilities, chemical industries and ships. The large-scale implementation of PCCC is, however, slowed by the difficulty of establishing business cases, partially due to operational costs of such technology. Relevant amongst the cost components is the solvent management costs, related to the degradation of the capture solvents. Aqueous amines suffer from degradation – oxidative and thermal – under different operating conditions in the capture plant [1].

Oxidative degradation of amines occurs due to the reaction of dissolved oxygen with the amines. This degradation is normally observed at temperatures below 100°C on CO<sub>2</sub>-loaded solvents. The oxidative degradation of amines leads to formation of several undesirable products like ammonia, carboxylic acids and aldehydes. While ammonia and aldehydes lead to increased emissions from the plant, the acidic products can further react with the amines forming heat stable salts (HSS) [2], [3]. The accumulation of these products in the solvent leads to reduction of cyclic capacity, and can cause increased fouling, corrosion and foaming. These issues make plant operation more difficult and expensive, in addition to having adverse environmental impacts.

Various techniques for mitigating oxidative degradation have been studied. Examples include removing dissolved oxygen by the use of oxygen scavengers, nitrogen sparging or membrane contactors [4]. Proper and effective application of these mitigation techniques requires an understanding of the extent and rate of oxidative degradation in various parts of the capture plant. This can be predicted using degradation models.

The degradation models currently proposed in literature follow a fundamental approach in which knowledge of degradation reactions and mechanisms is required [5]. Normally these models do not account for plant specific factors like residence times in various parts of the plant, quality of flue gas and plant operational profiles, leading to an inability to reasonably predict degradation in real plants.

Within the ALIGN-CCUS project, TNO started the development of a practical Degradation Network Model (DNM) aimed at prediction of the oxidative degradation of monoethanolamine (MEA) in the various operating units within a PCCC plant – absorber packing, absorber sump, piping between the absorber column and cross heat exchanger and in the cross heat exchanger. This model takes into account the plant specific factors mentioned above.

Within the LAUNCH project, the DNM has been updated, and further expanded to also predict degradation for CESAR1 (aqueous solution of 3 molar AMP and 1,5 molar piperazine). The current report describes the latest version of the model, the data used to estimate its parameters, and gives examples of the model application. Further DNM application exercises are carried out in WP6, as part of the techno-economic assessment of PCCC for multiple applications (waste-to-energy, coal-fired power, gas-fired power).

The DNM is a practical tool for predicting solvent quality overtime. As such, it allows for better selection and application of countermeasures to successfully operate of amine-based CO<sub>2</sub> capture plants, for a long term.

## 2 The DNM description

The degradation network model (DNM) is developed as a tool to predict oxidative degradation of solvents. Unlike fundamental degradation models, the DNM does not rely on knowledge of specific mechanisms of degradation, being easily adaptable to different amines. This empirical approach not only avoids the need to have an understanding of complex reaction mechanisms, but also makes the model independent on the degradation product matrix. Instead, the DNM is an empirical model relating the rate of degradation of a solvent to a generic solvent loss reaction, according to equation 1



where:

*DegP* refers to any degradation products formed; and

*a* is the stoichiometric coefficient defining how many mols of oxygen react per mol of amine.

As such, the rate of oxygen consumption is related to the rate of amine degradation as defined in equation 2:

$$\frac{d[O_2]}{dt} = -a \frac{d[\text{amine}]}{dt} \quad \text{eq.2}$$

The rate of oxygen consumption is assumed to be a function of the concentration of oxygen only, as the concentration of amine is somewhat constant, and considered to be present in large excess. The rate is then represented by eq. 3:

$$\frac{d[O_2]}{dt} = k[O_2]^n \quad \text{eq. 3}$$

where:

*n* is the order of reaction;

*k* is the kinetic constant, in mol<sup>0.5</sup>.L<sup>0.5</sup>.h<sup>-1</sup>

The order of reaction, determined in this work with basis on experimental data (see chapter 3) to be equal to 0.5. The kinetic constant is considered to be an Arrhenius function, as defined in eq.4:

$$k = k_0 e^{E_a/RT} \quad \text{eq. 4}$$

where:

*k<sub>0</sub>* is the pre-exponential factor, in mol<sup>0.5</sup>.L<sup>0.5</sup>.h<sup>-1</sup>;

*E<sub>a</sub>* is the activation energy, in J.mol<sup>-1</sup>.

In this way, the rate of oxygen decay, which can be measured, can be correlated to the expected amine losses due to oxidative degradation. The oxygen decay experimental data used to derive the kinetic constant ( $k_0$  and  $E_a$ ) are generated using a lab installation, the oxygen depletion installation (ODIN), as described in chapter 3.

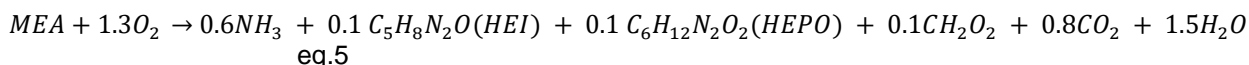
The stoichiometric factor  $a$  is estimated based on long-term degradation data obtained at the RWE pilot plant for both MEA and CESAR1 solvents.

## 2.1 Comparison with other models available in literature

### 2.1.1 Léonard et al., 2014

Léonard et al. [6] proposed a kinetic model for the prediction of MEA degradation. The authors have used a semi flow batch reactor, in which a gas flowed through the reactor, whereas there is no liquid flow. A typical experiment lasted for 21 days. The study quantified the influence of the temperature (55, 100, 120 and 140°C) and of the O<sub>2</sub> (5, 7.5 and 10 vol%) and CO<sub>2</sub> (7.5, 15, 30 vol%) concentrations in the gas feed are studied, and their effect on the MEA loss and the formation of degradation products.

The authors described the MEA degradation through an apparent reaction, given in eq. 5. This is similar to DNM's eq.1, and suggests a stoichiometric factor of 1.3 mol O<sub>2</sub> per mol MEA reacted. The stoichiometric factors are assigned based on observed distribution of degradation products during the experiments.



Based on that, the authors have come to expression for the MEA oxidative degradation rate given in eq.6:

$$-r_{MEA} = 5.35 \times 10^5 e^{-41.730/RT} [O_2]^{1.46} \quad \text{eq. 6}$$

where:

$R$  is the universal gas constant, 8.314 J.mol<sup>-1</sup>.K<sup>-1</sup>;

$T$  is the temperature, in K;

the value for  $E_a$  is given in J.mol<sup>-1</sup>;

the value of  $k_0$  is given in in mol<sup>0.46</sup>.L<sup>0.46</sup>.s<sup>-1</sup>;

$[O_2]$  is the oxygen concentration in water, in mol.L<sup>-1</sup>.

Only one experiment was conducted at the low temperature range, 55°C, for which the CO<sub>2</sub> concentration in the feed gas was 15 vol%. At these conditions, an equilibrium loading of 0.52 mol/mol is expected. In real operations, along the absorber column height, the loadings will typically vary between ca. 0.2 and 0.5 mol/mol. And temperatures typically vary between 40°C and 60-70°C.

The other 10 experiments are conducted at 100-140°C. The lower boundary, 100°C is achieved in the cross-heat exchanger, and for MEA it is usual to limit the reboiler temperature to 120°C to avoid substantial thermal

degradation. It can be argued that, once the solvent reaches the stripper, any dissolved oxygen is stripped by the vapor/CO<sub>2</sub> upflow immediately, which prevents oxidation from happening. Therefore, in the hot rich solvent line, desorber packing and sump and reboiler, the solvent is not expected to be exposed to oxygen [7].

Therefore, it is possible that the kinetic parameters and stoichiometric relationships generated in this study are not the most representative of the oxidative degradation taking place in the cold side of the plant (absorber packing and sump, and rich line all the way to the cross heat exchanger).

### 2.1.2 Pinto et al., 2014

The modelling work of Pinto et al. [5] benefited from an extensive set of degradation data, reported in Vevelstad et al.[8], also produced in a semi flow batch reactor (SFBR). The initial MEA concentration used in the tests was 30 wt%, and it was pre-loaded with 0.4 mol<sub>CO<sub>2</sub></sub>/mol<sub>MEA</sub> (thus more representative of the lower section of the absorber). The oxygen concentration in the gas inlet varied between 6 and 98 vol%, to lead to accelerated degradation, and the temperature was representative of the absorber, varying between 55 and 75 °C.

The model proposed is based on fundamental mass balance applied over the SFBR, taking into consideration mass transfer between the gas and the liquid, and a set of 8 reactions describing the formation of formaldehyde, formic acid, glyoxal, oxalic acid, N-(2-hydroxyethyl) formamide (HEF), N-(2-hydroxyethyl) imidazole (HEI), N,N'-bis(2- hydroxyethyl) oxalamide (BHEOX), N-(2- hydroxyethyl) glycine (HEGly) and ammonia.

While the model could represent the experimental data with relative success, the approach requires knowledge on specific degradation routes. This makes it hard to extend the model to different solvents. Moreover, the relatively high degree of complexity leads to difficulties to implement the model of Pinto et al. in simulators.

### 3 Lab scale degradation data: ODIN experiments

The ODIN setup (Oxygen Depletion INstrument) allows for determining the oxygen consumption rate in a solvent. The effect of temperature and CO<sub>2</sub> loading, as well as other factors such as metal content, can be assessed in the ODIN. The set-up was designed, constructed and operated by TNO, to generate the data required to estimate the DNM parameters.

#### 3.1 ODIN description

The ODIN setup is shown in Figure 1. ODIN has two reaction vessels inside a glovebox which would be filled with N<sub>2</sub> to prevent air leaking into the vessels. The vessels are jacketed and connected to a water bath which allows for temperature control. While the two vessels can be seen in the picture (Figure 1, left), only one vessel is shown in the schematic representation (Figure 1, right) for sake of simplicity.

At the start of an experiment, the vessels are completely filled with solvent with the desired concentration and CO<sub>2</sub> loading. The solvent is then loaded with O<sub>2</sub> (using compresses air or pure oxygen) up to the equilibrium point. The vessels are then tightly closed. It should be noted that there is no head space in the vessels – hence, there's only a liquid phase. The liquid is continuously stirred by magnetic stirrers. The vessel top lid has connections through which a thermocouple and an oxygen sensor are inserted into the liquid. The thermocouple is used to control the temperature of the water bath.

The oxygen concentration is measured using an Endress-Hauser Liquiline CM448 with Memosens COS81D Optical Oxygen sensor. The sensor is connected to a datalogger and records dissolved oxygen levels in mg/L every 30 seconds.

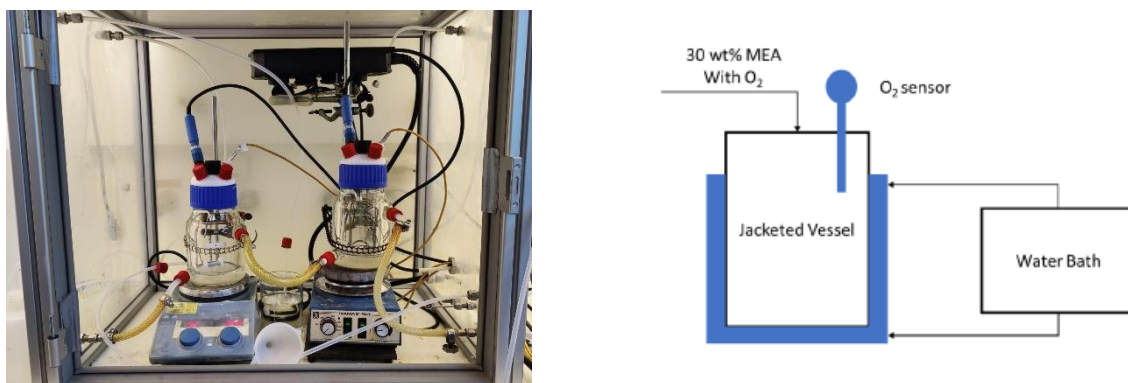


Figure 1. ODIN setup. Left: picture; Right: schematic representation

##### 3.1.1 Chemicals

The chemicals used in these experiments were as follows: Monoethanolamine (Sigma-Aldrich/Thermoscientific) (98%), Monoethanolamine (Brenntag) (98%), 2-amino-2-methyl-1-propanol (Thermoscientific) (90%), piperazine (Thermoscientific) (99%). AMP (26,72wt%) and piperazine (12,97wt%) were used formulate the CESAR1 solvent.

### 3.1.2 Experimental method

To perform an experiment 800 grams of described solvent was loaded with CO<sub>2</sub> on a scale to a previously calculated amount of absolute mass (and confirmed with FTIR). This solution was then loaded into the vessels and sparged for 10 minutes with pure oxygen at 60l/h. The headspace of the vessel is filled up and the O<sub>2</sub> sensor removed and reinserted to avoid trapped air bubbles. After this the measurement was started and took up to a maximum of 24 hours. These tests were carried out at different temperatures and CO<sub>2</sub> loadings.

### 3.2 ODIN results for MEA and discussions

ODIN tests were carried out to measure the decay of oxygen in 30 wt% MEA at different CO<sub>2</sub> loadings and temperatures to reflect absorber conditions. To properly observe the decay of oxygen in MEA, the experiments were carried out with pure oxygen. An overview of the experimental conditions is provided in Table 1. Experiments 1-7 were previously reported in D2.1.2, but are also included here for sake of completion.

Table 1. Experimental matrix for ODIN tests with 30 wt% MEA

Experiment ID	CO <sub>2</sub> Loading (molCO <sub>2</sub> /molMEA)	Temperature (°C)
1	0	40
2		50
3		60
4	0.24	40
5	0.27	
6	0.4	
7	0.5	
8	0.2	20
9		40
10		50
11	0.3	20
12		40
13		50
14	0.5	20
15		40
16		50

In experiments 1 to 3, oxygen decay was observed in unloaded 30 wt% MEA at temperatures between 40°C and 60°C. It was observed that the rate of decay was relatively low and did not increase significantly when increasing temperature. The amount of dissolved oxygen decreased with increasing temperature as expected. These results can be seen in Figure 2, which shows the rate of oxygen consumption which correlates with the degradation of the solvent via eq.1.

In the next set of experiments (4 to 7), oxygen decay was observed as a function of CO<sub>2</sub> loading at 40°C. As shown in Figure 2, the introduction of CO<sub>2</sub> into the system significantly increases the rate of oxygen consumption. However, for the loading range investigated in these experiments, the rate of oxygen consumption is seen to be higher for lower loadings and decreases as the loading increases.

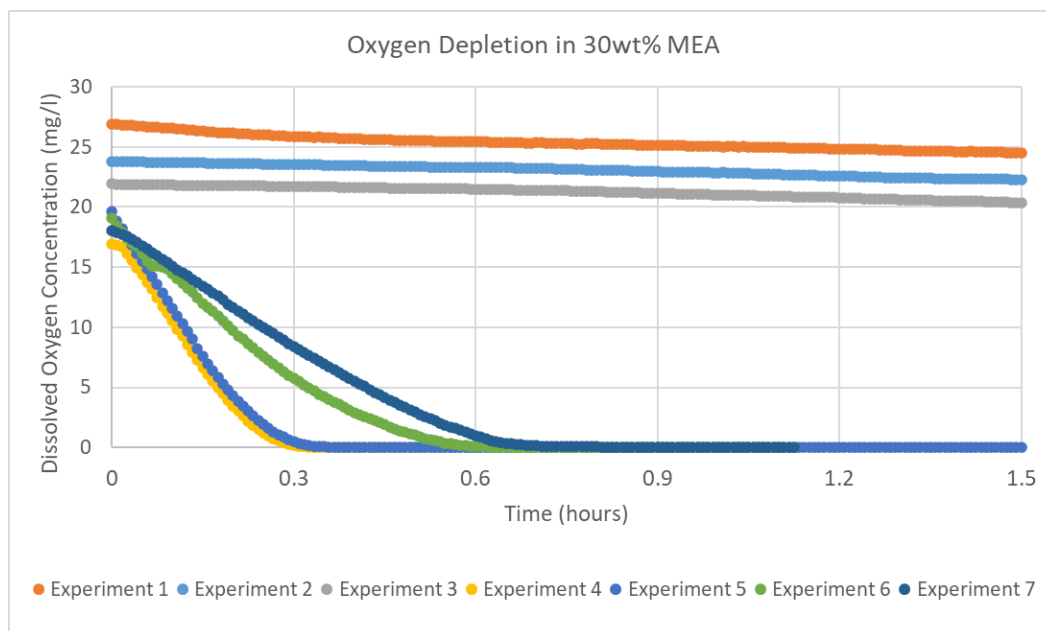


Figure 2. Oxygen decay in 30 wt% MEA. For experiments settings, please refer to Table 1

Experiments 8-10, 11-13 and 14-16 were performed by varying the temperature (20°C, 40°C and 50°C) with CO<sub>2</sub> loadings of 0.2, 0.3 and 0.5 respectively.

Figure 3 (a, b and c) shows the rate of oxygen consumption, which correlates with the degradation of the solvent via eq.1. The higher the temperature, the faster the degradation of the solvent. The figure also evidences a decrease in oxygen solubility with increased temperature.

In agreement to what was observed in experiments 4-7, Figure 3d shows that at lean loading the degradation rate is faster than at rich loading range. While Figure 3d only shows data for 40°C, for simplicity, the same trend is also observed at 50°C. For unloaded systems the degradation is very slow, but it greatly accelerates once the solvent is loaded. At a certain point, which seems to be between 0,3 and 0,5 mol CO<sub>2</sub>/mol for 30 wt% MEA, the degradation starts to slow down with loading. This shift in behavior is evidenced in Figure 4, where the time it took for the solution to degrade (arbitrarily defined here as reaching DO concentration below 1 mg/L) is plotted as a function of loading. For unloaded solutions, the experiments were terminated at 24h, before achieving the low DO limit.

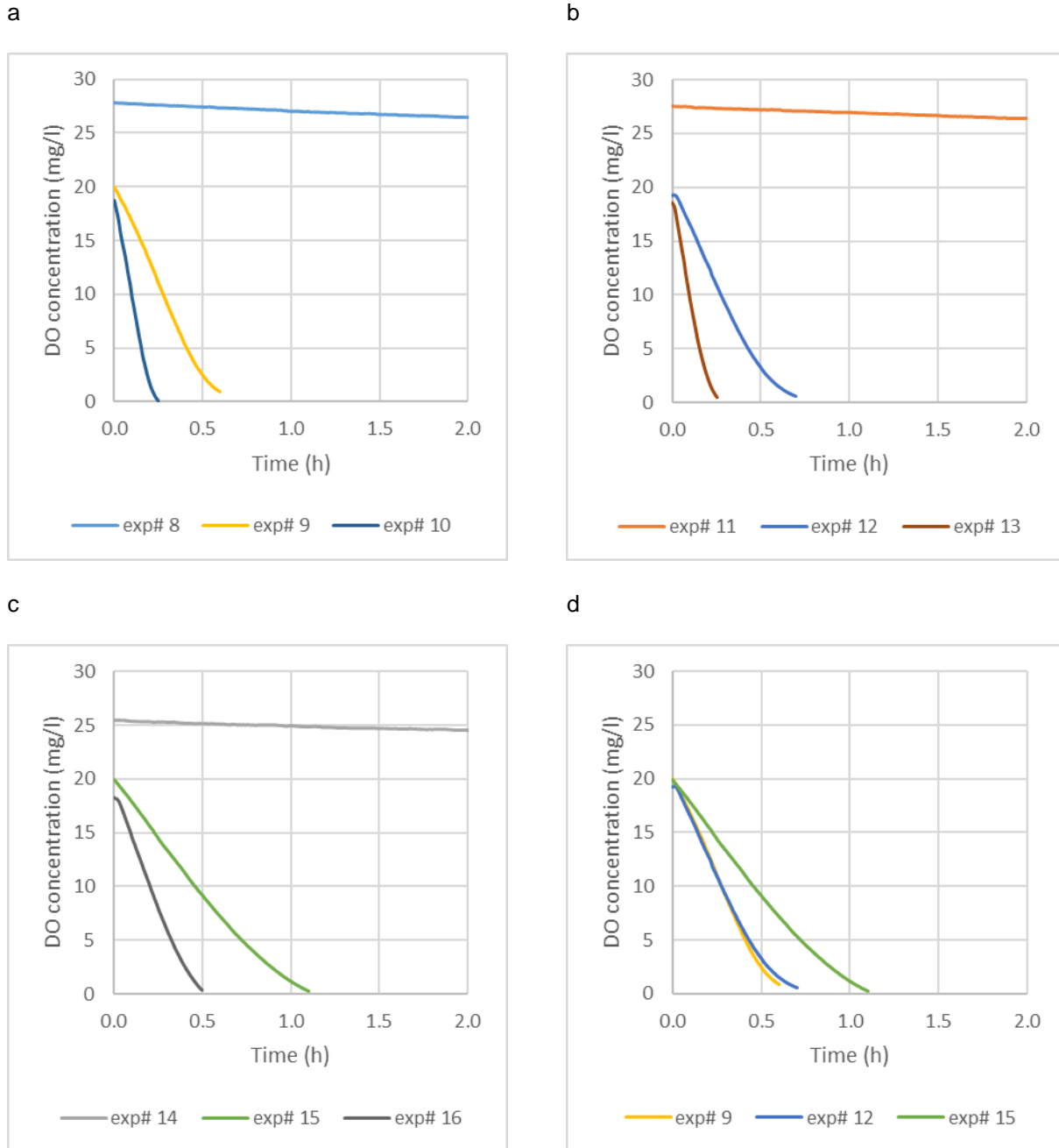


Figure 3. ODIN data for oxygen consumption in MEA, experiments 8-16. For experiments settings, please refer to Table 1

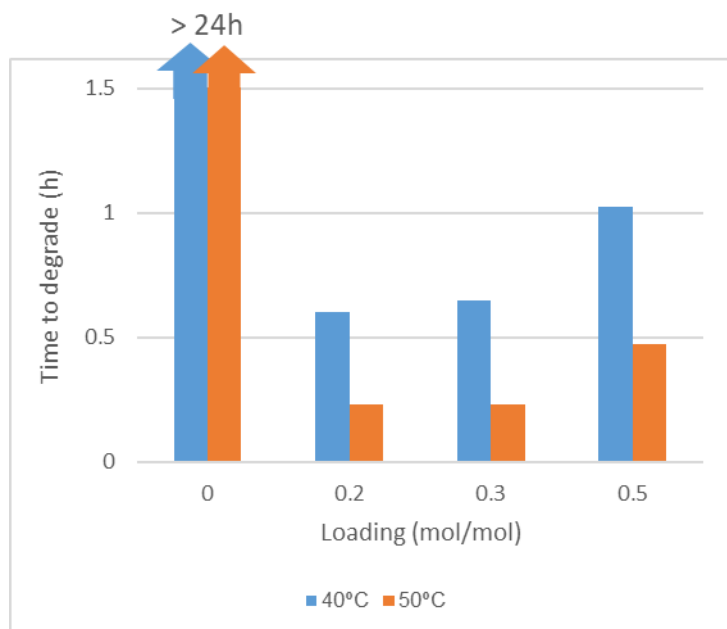


Figure 4. Time to degrade (reach  $DO < 1\text{mg/L}$ ) for 30wt% MEA as a function of loading

Supap et al. [3] have reported decreased degradation rate with increased loading. In their work, unloaded MEA degraded faster than loaded. The authors have therefore attributed their observation to salting out of oxygen when loading increases. It should be stressed that in the work by Supap et al, the overall loss of MEA was measured over time as opposed to oxygen decay.

Our work indicates that factors other than oxygen solubility have an impact on the oxygen consumption rate. One could conjecture that a different mechanism takes place once the solvent is loaded (MEA carbamates or protonated MEA could be more prone to degradation than molecular MEA). However, if this would be the case, one would expect the oxygen decay to increase with increasing loading, which is only observed in the transition between 0 and 0.2 loading. At the transition between 0.3 and 0.5 loading, the opposite is observed.

All experiments were executed – at least – in duplos, and the results presented in here are reproducible. With the current evidence, we cannot offer a fundamental explanation to these observations. For that, more data should be generated, with more loadings being tested, particularly between 0-0.2 and 0.3-0.5. From a practical perspective, the loading region between 0.2-0.5 is of most relevance, which could help guide the experimental planning of future campaigns. But from a fundamental perspective, also loadings above 0.5 could be explored (notice that the current ODIN version does not allow for high pressure operation).

### 3.3 Results for CESAR1

Similar to MEA, ODIN tests were carried out to measure the decay of oxygen in CESAR1 at different CO<sub>2</sub> loadings and temperatures to reflect absorber conditions. The experiments were carried out with pure oxygen, at 40°C, 50°C and 60°C with four different levels of CO<sub>2</sub> loading: 0, 0.1, 0.3 and 0.4 molCO<sub>2</sub>/mol<sub>amine</sub>. An overview of the experimental conditions is provided in Table 2. The loading is defined as the ratio between the moles of CO<sub>2</sub> and the sum of the moles of both amines. CESAR1 concentration is 3M AMP and 1,5M PZ, so a loading of 0.1 molCO<sub>2</sub>/mol<sub>amine</sub> means that 0.45M of CO<sub>2</sub> has been absorbed by the sample.

Table 2. Experimental matrix for ODIN tests with CESAR1

Experiment ID	CO <sub>2</sub> Loading (molCO <sub>2</sub> /mol <sub>amine</sub> )	Temperature (°C)
17	0	40
18		50
19		60
20	0.1	40
21		50
22		60
23	0.3	40
24		50
25		60
26	0.4	40
27		50
28		60

The results of experiments 17-28 are given in Figure 5. Attention is drawn to the fact that the graphs show the ODIN data for a period of 20 hours, whereas the data presented for MEA was for 2 hours. Figure 5 a, b, c and d presents all data obtained at loadings 0, 0.1, 0.3 and 0.4, respectively. In all cases, oxygen solubility decreases and degradation rate increases with increasing temperature.

To better visualize the effect of loading, experiments 17-28 are re-grouped by temperature in Figure 6. Figure 6a shows that, at 40°C, the rate of oxygen decay is much faster at loading 0.1 than at any other loading tested (0, 0.3 and 0.4 curves have very similar slope). The same trend is observed in Figure 6b showing 50°C data. Interestingly, at 60°C (Figure 6c), all loadings lead to accelerated degradation as compared to unloaded data. The loading of 0.1 has a slightly more pronounced effect than 0.3 or 0.4.

At the moment, we don't see a clear explanation for this behavior. But at least on a qualitative basis, this is similar to what is observed for MEA: there is a shift in the degradation rate as a function of loading. More data is required before any explanation could be offered.

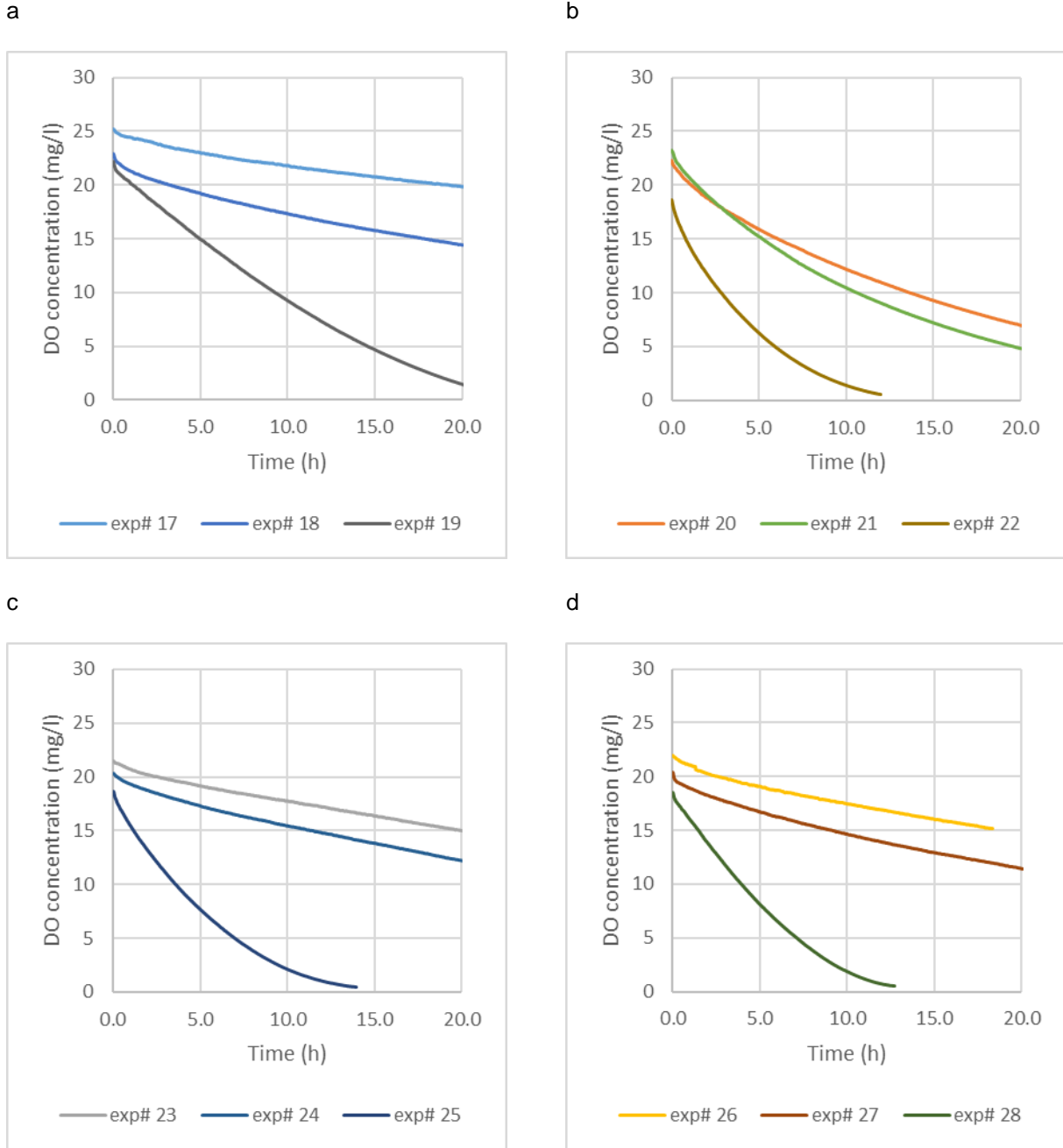
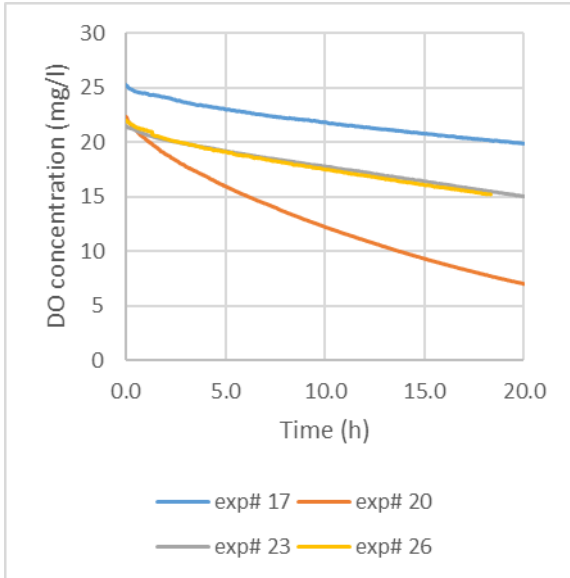
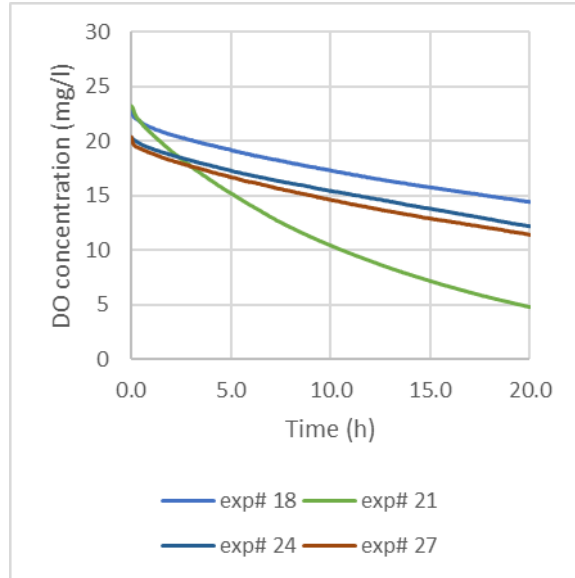


Figure 5. ODIN data for oxygen consumption in CESAR1, experiments 17-28, grouped by loading. For experiments settings, please refer to Table 2

a



b



c

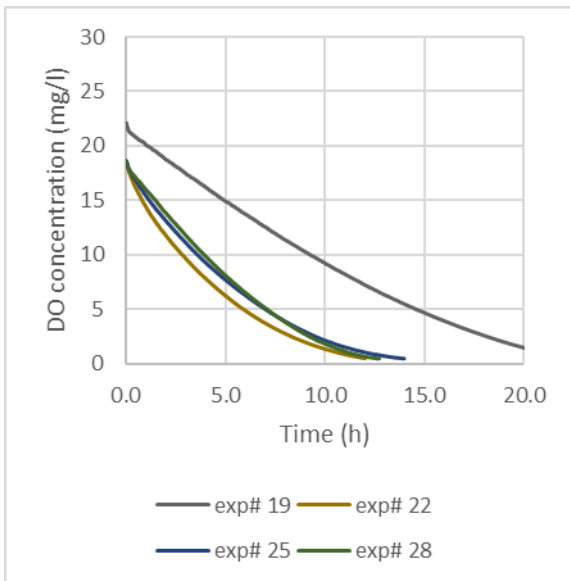


Figure 6. ODIN data for oxygen consumption in CESAR1, experiments 17-28, grouped by temperature. For experiments settings, please refer to Table 2

### 3.4 Deriving order of reactions and kinetic parameters

#### 3.4.1 Order of reaction – MEA and CESAR1

The rate expressions used in this work are given in eq. 3. The order of reaction,  $n$ , must be determined based on the obtained ODIN data. In order to do so, different orders of reaction were screened, from 0 to 0.2. The value of 1.46, as proposed by Léonard et al. [6] (see eq.6), was also included in this screening. The rate expression and its integrated form as a function of the order of reaction can be seen in Table 3. The integrated form is always a linear equation ( $y = ax + b$ ) with the independent variable being time, and the dependent variable some transformation of the oxygen concentration (e.g.,  $\ln[O_2]$  for order 1). When plotting  $y$  against  $x$ , the slope is a function of the kinetic constant, and the intercept is related to the initial oxygen concentration,  $[O_2]_0$ . To better visualize the results, in **Error! Reference source not found.** and Figure 7, we have plotted  $y - b$  against  $x$  (therefore all graphs have zero as intercept).

In **Error! Reference source not found.**, the data for 40°C and 0.3 mol/mol loading is analysed, and it can be seen that a half-order reaction leads to the best fit. This was also observed for the remainder of the ODIN data for MEA, and the order of reaction is then set to 0.5. In Figure 8, the data for 60°C and 0.3 mol/mol loading is analysed, and it can be seen that a half-order reaction leads to the best fit. This was also observed for the remainder of the ODIN data for CESAR1, and the order of reaction is then also set to 0.5.

Table 3. Rate expression and its integrated form as a function of order of reaction

Order of reaction	Rate expression	Integrated rate law
0	$r = -k[O_2]^0$	$[O_2] = -kt + [O_2]_0$
0.5	$r = -k [O_2]^{0.5}$	$[O_2]^{0.5} = -\frac{1}{2}kt + [O_2]_0^{0.5}$
1	$r = -k [O_2]$	$\ln[O_2] = -kt + \ln[O_2]_0$
1.46	$r = -k [O_2]^{1.46}$	$\frac{1}{[O_2]^{0.46}} = 0.46kt + \frac{1}{[O_2]_0^{0.46}}$
2	$r = -k [O_2]^2$	$\frac{1}{[O_2]} = kt + \frac{1}{[O_2]_0}$

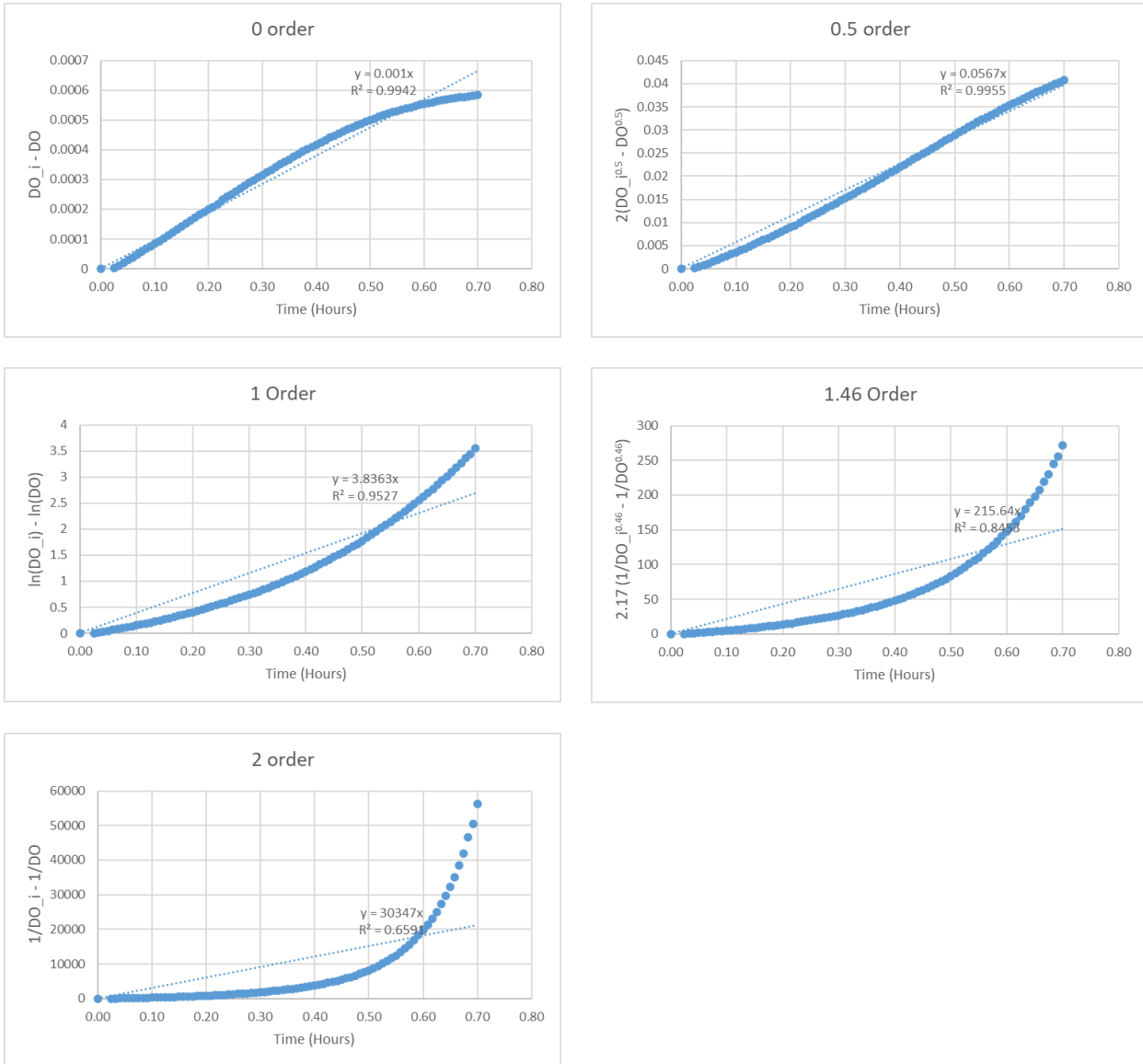


Figure 7. Order of reaction analysis, using ODIN data for 30wt% MEA at 40°C and loading 0.3 mol/mol

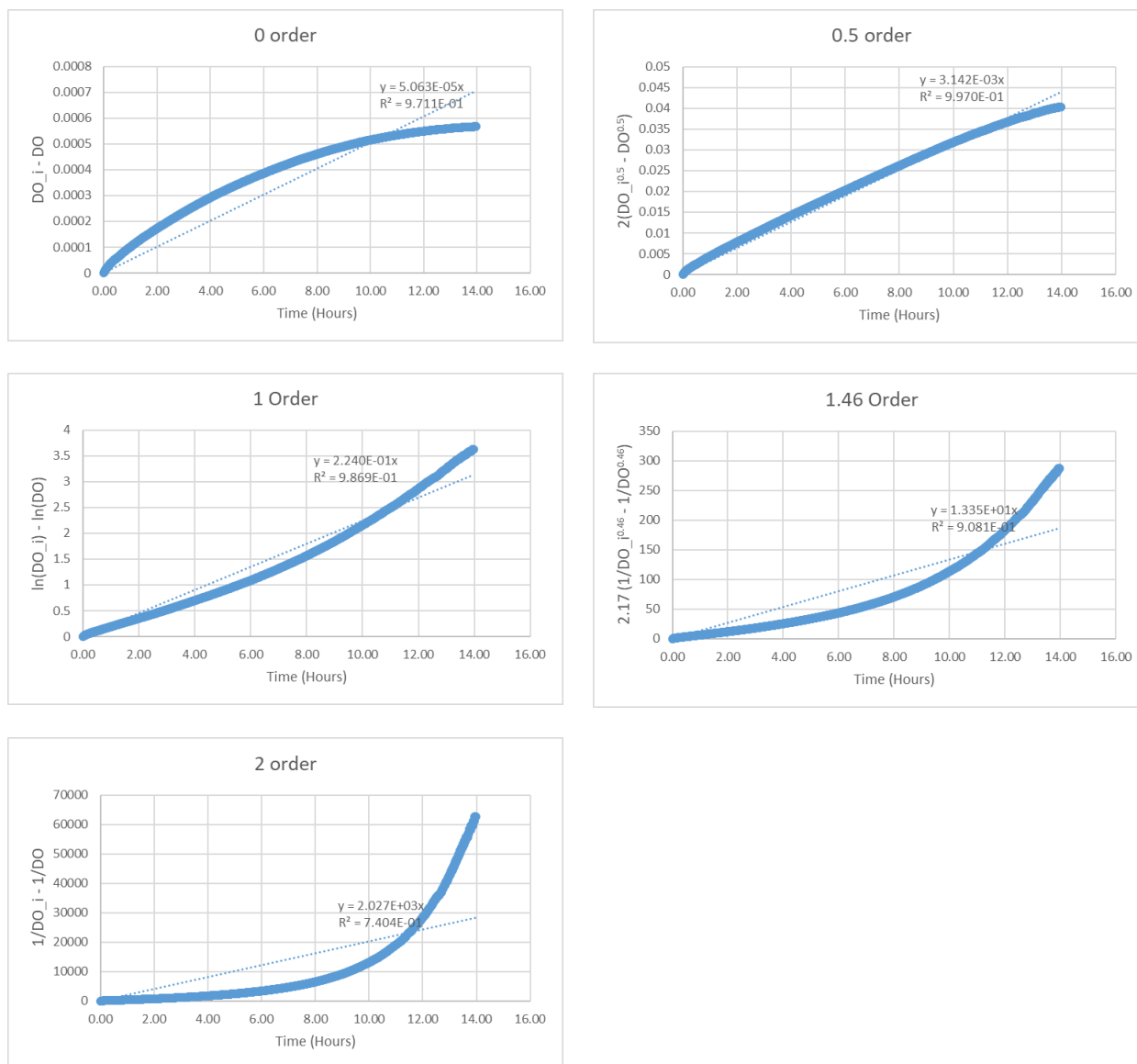


Figure 8. Order of reaction analysis, using ODIN data for CESAR1 at 60°C and loading 0.3 mol/mol

### 3.4.2 Kinetics parameters – MEA

Having set the order of reaction at 0.5, the kinetic constant could be determined for all loadings and temperatures, and this data is given in Table 4 for MEA.

Table 4. Estimated kinetic constant ( $\text{mol}^{0.5} \cdot \text{L}^{0.5} \cdot \text{h}^{-1}$ ) as a function of temperature and loading

T (°C)	Loading (mol/mol)		
	0.2	0.3	0.5
20	6.00e-4	5.00e-4	4.00e-4
40	6.14e-2	5.67e-2	3.58e-2
50	1.61e-1	1.55e-1	7.47e-2

For each of the loadings, the pre-exponential factor and activation energies are then calculated. For that, eq. 4 is linearized to eq. 7. Then, by plotting  $\ln k$  against  $1/T$ , one obtains a line where  $\ln k_0$  in the intercept and  $E_a/R$  is the slope.

$$\ln k = \ln k_0 + E_a/RT \quad \text{eq. 7}$$

Table 5. Estimated kinetic parameters as a function of loading

Parameter	Unit	Loading (mol/mol)		
		0.2	0.3	0.5
$E_a$	$\text{J} \cdot \text{mol}^{-1}$	8.12e4	8.46e4	6.19e4
$k_0$	$\text{mol}^{0.5} \cdot \text{L}^{0.5} \cdot \text{h}^{-1}$	2.12e12	7.21e12	7.53e8

In order to apply the DNM model, the oxygen reaction rate needs to be a continuous function of loading. To illustrate the impact of the function choice, three functions are suggested in Figure 9 for each kinetic parameter. Function 1 is a linear interpolation between the existing data points. The logic to build function 2 is: if loading < 0.45 then linearly interpolate/extrapolate the parameters using the values for 0.2 and 0.3 loading as basis. Otherwise, fix the parameters at the loading 0.5 value. Finally, function3 is a second order polynomial fit. With this limited set of data, there's no clear way of choosing between the different functions presented. A second order polynomial fit (function 3) suggests shifts in behavior around loading 0.3. However, it could be possible that the kinetic parameters are a linear function of loading between 0.2 and 0.45, and drop steeply between 0.45 and 0.5, as suggested by function 2. The point here is not to conclude on which function would be a better representation of reality, but simply illustrate that, with both kinetic parameters being strong functions of loading, there is a need to obtain more experimental data in order to refine the DNM.

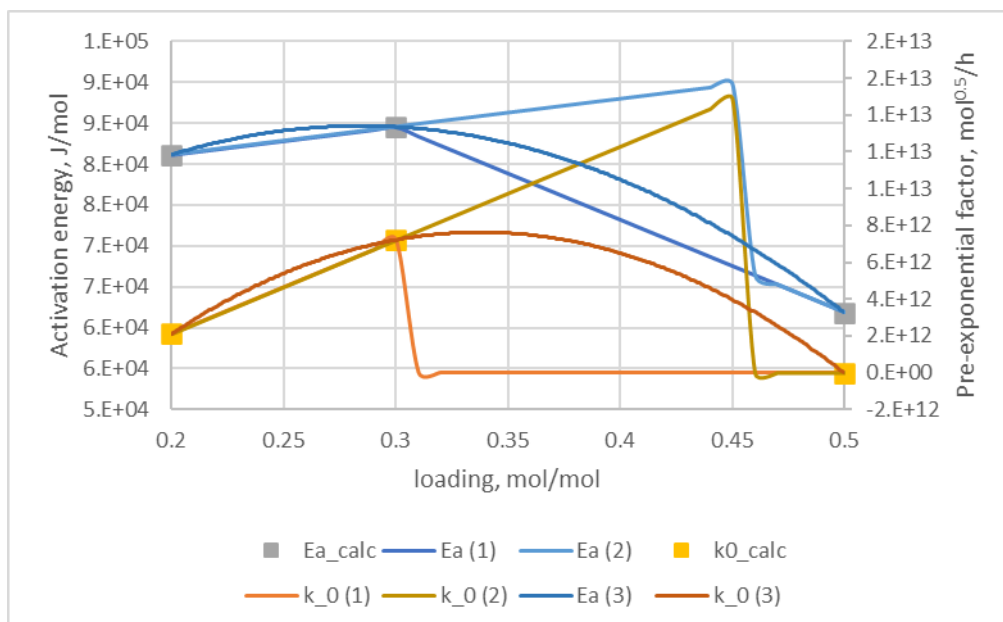


Figure 9. Continuous functions to calculate activation energy and pre-exponential factors, and calculated values as reported in Table 5

### 3.4.3 Kinetics parameters – CESAR1

Having set the order of reaction at 0.5, the kinetic constant could be determined for all loadings and temperatures, and this data is given in Table 6 for CESAR1.

Table 6. Estimated kinetic constant ( $\text{mol}^{0.5} \cdot \text{L}^{0.5} \cdot \text{h}^{-1}$ ) as a function of temperature and loading

T (°C)	Loading (mol/mol)			
	0	0.1	0.3	0.4
40	3.31e-4	1.04e-3	4.25e-4	5.30e-4
50	5.98e-4	1.56e-3	5.93e-4	6.77e-4
60	1.93e-3	3.36e-3	3.14e-3	3.27e-3

For each of the loadings, the pre-exponential factor and activation energies are then calculated using eq. 7.

Table 7. Estimated kinetic parameters as a function of loading

Parameter	Unit	Loading (mol/mol)		
		0.1	0.3	0.4
$E_a$	$\text{J} \cdot \text{mol}^{-1}$	3.45e4	2.82e4	2.06e4
$k_0$	$\text{mol}^{0.5} \cdot \text{L}^{0.5} \cdot \text{h}^{-1}$	5.28e2	2.12e1	1.46e0

As for MEA, both kinetic parameters are strong functions of loading, thus reinforcing the need to obtain more experimental data in order to refine the model. Moreover, in CESAR1 operations a maximum loading of 0.6-0.7 is expected, so data in the higher loading range is needed to refine the model.

For CESAR1, representing the kinetic parameters as continuous function of loading is even more challenging, as it requires extrapolation. The estimated activation factor is arbitrarily estimated by linear inter- and extrapolation, as represented in Figure 10.

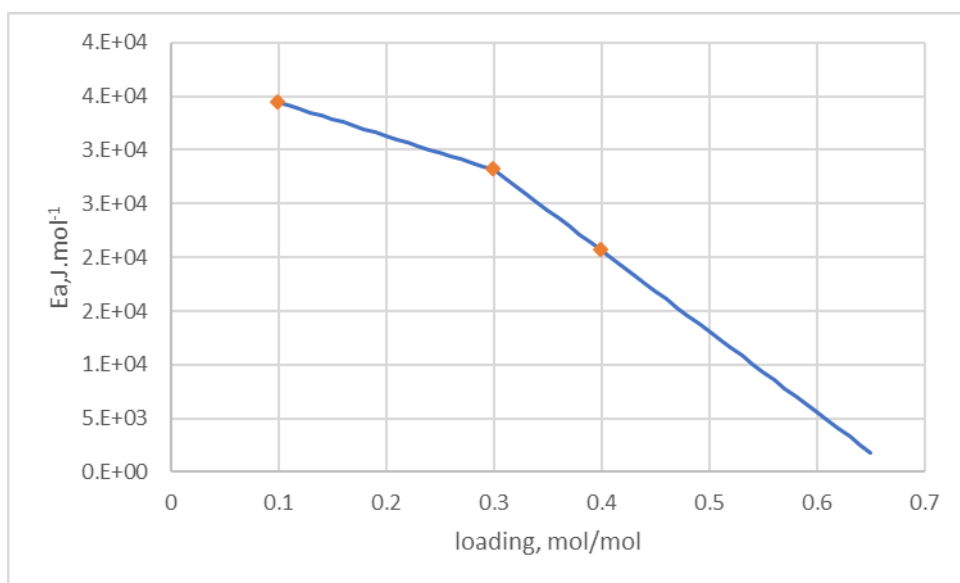


Figure 10. Continuous function to represent the pre-exponential factor for CESAR1. Data points (orange diamonds) are given in Table 7

When it comes to the pre-exponential factor, linear extrapolation beyond 0.4 would lead to negative values. Therefore, another arbitrary function is proposed. The calculated values are represented in Figure 11 (notice the y axis in log scale). Between loadings 0.1 and 0.3, the pre-exponential factor declines linearly. Between 0.3 and 0.55, it retains the value estimated at loading 0.4 ( $1.46 \text{ mol}^{0.5} \cdot \text{L}^{0.5} \cdot \text{h}^{-1}$ ). And above 0.55, a new fixed value of  $0.46 \text{ mol}^{0.5} \cdot \text{h}^{-1}$  is set. It is not physically likely that the pre-exponential factor will be constant at a certain loading ranges and behave as a step function; at best, the values calculated give a reasonable indication of the order of magnitude of the parameter.

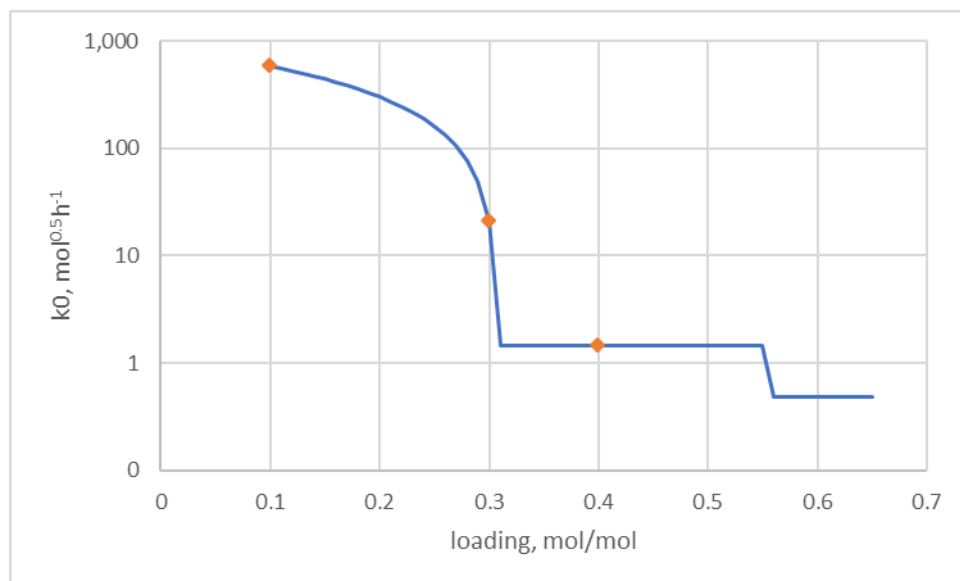


Figure 11. Continuous function to represent the pre-exponential factor for CESAR1. Data points are given in Table 7

### 3.5 DNM limitations

The current version of the DNM only takes into consideration amine losses due to direct reaction with oxygen. As such, reactions of MEA or oxygen with degradation products are discarded. It is known, for instance, that MEA reacts with glyoxylic acid to form N-(2-hydroxyethyl)-glycine (HEGly), and that formic acid is a result of the reaction between formaldehyde and oxygen [8]. The data based on which the kinetic parameters of the DNM model is performed with fresh amine solutions. The average duration of an experiment is 24h. Within this period, while the oxygen consumption is quite relevant (and in many cases complete), the amine content in the solvent remains practically unchanged. The concentration of degradation products after one experiment, while not measured, is expected to be in ppb-ppm levels, as opposed to 4,5 to 5 M concentration of amines used in the tests (for CESAR1 and MEA, respectively). As such, it is much more likely that oxygen will react directly with the amines, present in concentrations many orders of magnitude higher than their degradation products. In long-term plant operations, degradation products accumulate in the solvent system. It is likely that the ODIN data obtained with fresh solvent is not representative of the degradation rate of more extensively solvents.

The ODIN data that forms the basis of the DNM model was obtained between 20 and 50°C for MEA, for loadings 0-0.5. For CESAR1, the loading range was 0-0.4, and the temperature 40-60°C. It is important to increase the temperature range to ca. 100°C, in order to better represent all unit operations in the plant all the way up to the hot rich piping between the cross heat exchanger and the stripper inlet. For CESAR1, the loading range must be extended to at least 0.7 mol/mol. And for both solvents, more data at varying loadings would allow for proposing a continuous model to represent the kinetic parameters as a function of loading.

Moreover, the DNM is derived from ODIN data performed with fresh, metal-free solvent. In reality, the solvent matrix will include degradation products, impurities from the flue gas as well as metals originated via corrosion of the materials of construction. Additionally, no thermal degradation losses are considered in the DNM.

## 4 DNM application

### 4.1 Base case: the ALIGN-CCUS WtE case

In the ALIGN-CCUS project, a reference case for CO<sub>2</sub> capture from the flue gas of a waste incinerator process was defined. A capacity of 200 kton of waste per year was considered, representing the European average waste incinerator. The reference plant was simulated, and the estimated flue gas output was 49.8 kg/s, with a CO<sub>2</sub> content of 9.8 vol% (resulting in 212 kton of CO<sub>2</sub> emitted per year). Two CO<sub>2</sub> capture solvents were considered in ALIGN-CCUS: 30 wt% MEA and CESAR1. For these solvents, a conceptual design of a CO<sub>2</sub> capture plant was proposed, having 90% capture rate as target. That study is presented in ALIGN-CCUS public report D1.4.3 "Guidelines and Cost-drivers of capture plants operating with advanced solvents".

The AVR waste-to-energy (WtE) company is a partner in LAUNCH. AVR has two waste incinerators in operation in The Netherlands: Duiven and Rozenburg. The two WtE plants combined emitted ca. 1.1 Mt<sub>CO<sub>2</sub></sub>, of which 60% or 659 kt<sub>CO<sub>2</sub></sub> was biogenic [9]. Therefore, an average of 220 kt<sub>CO<sub>2</sub></sub> of fossil-based CO<sub>2</sub> was emitted per plant. With these numbers in mind, it was decided that the ALIGN-CCUS scale was relevant also for LAUNCH, and that existing model was used as a base case to apply the DNM.

### 4.2 DNM applied to MEA and CESAR1 WtE capture plants

To apply the DNM, information on temperature, loading and residence time on each of these segments is used to calculate the oxygen consumption. Using the DNM and the process data obtained from the performed ProTreat® simulations, the total oxidative degradation rate can be estimated for the different segments of the plants. In this work, the absorber packing, the absorber sump and the cross heat exchanger are considered.

#### 4.2.1 Setting the stoichiometric factor: RWE data

In order to translate the oxygen consumption into solvent consumption, the stoichiometric factor,  $\alpha$  is needed. This factor was treated as a fitting parameter, and used to achieve a target degradation rate. The target degradation rates were defined based on RWE pilot results.

From the RWE pilot operations with MEA, the total MEA consumed was 210 gMEA/tonCO<sub>2</sub> captured during the first 55 days of operation, and increased to 350 gMEA/tonCO<sub>2</sub> captured when taking the first 288 days of operation into account. These solvent losses are mostly due to degradation, as emissions were kept very low during the operational periods in question. During the CESAR1 operations at the RWE pilot, some aerosol-based emissions were experienced which have a significant contribution to solvent losses. At an operational interval, a dry bed was included in the absorber operation, which greatly lowered solvent emissions. The solvent losses during that period, 150 gCESAR1/tonCO<sub>2</sub> captured are considered as the baseline for this solvent.

Figure 12 shows the calculated MEA and CESAR1 consumption estimated in the reference WtE plant, as a function of the stoichiometric factor. Initially, a value of 1.3 was used, as suggested by Léonard for MEA [6]. That lead to low consumption when compared to RWE. By adjusting the factor to 0.69 in the case of MEA and 0.32 in the case of CESAR1, the target degradation rates of 210 and 150 g/tonCO<sub>2</sub> could be achieved, respectively.

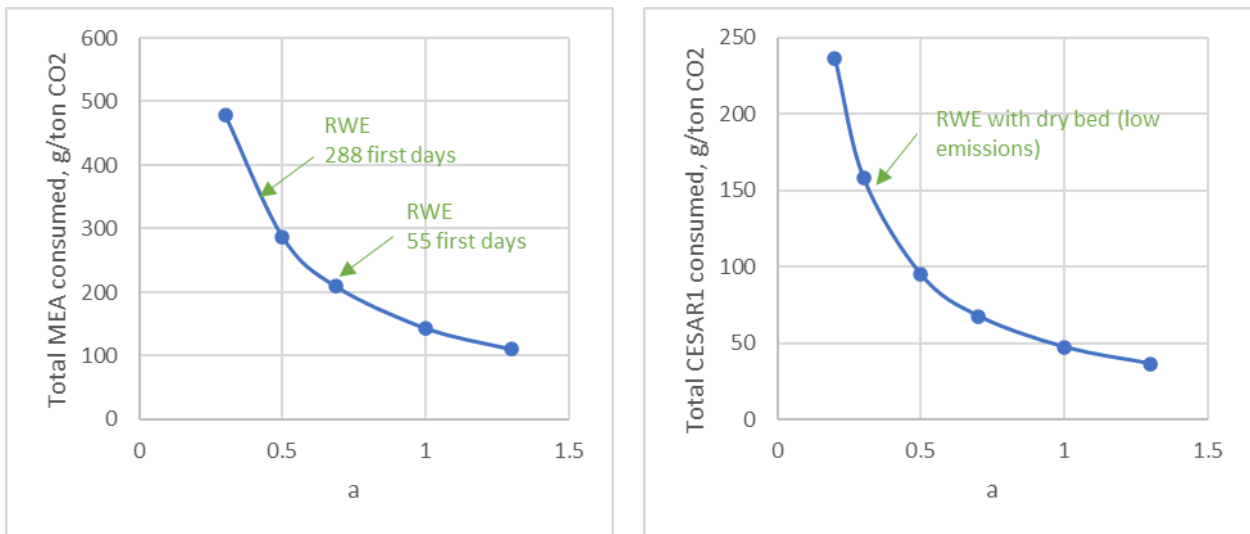


Figure 12. MEA and CESAR1 consumption as a function of stoichiometric factor “a”.

By treating the stoichiometric factor as a fitting parameter, we are able to anchor the DNM model results to real plant data results. This allows us to compensate for the DNM limitations, discussed in section 3.5. On the other hand, the factor loses its physical meaning – i.e., it can no longer be interpreted as a stoichiometric factor, and a direct comparison between the values in this work and those in literature is no longer possible.

In refining the DNM, for instance by generating more ODIN data as to improve the kinetics parameters estimations, the future DNM version will require a refit of the factor “a”. When the kinetics are representative of a solvent matrix in an operational plant, than “a” should regain its physical meaning.

#### 4.2.2 Absorber packing – MEA

As discussed, in order to apply the DNM, the kinetic parameters need to be represented by a continuous function of loading. For the present application, it was decided to use function 2 reported in Figure 9. Applying this logic and the factor “a” of 0.69, the MEA consumption over the packing can be calculated, as given in Figure 13d.

The conceptual design considers an absorber packing height of 18m, with an intercooler at the lower packing section (13m packing depth). In the ProTreat simulation, the absorber packing is discretized into 27 segments, and for each segment a liquid temperature (Figure 13a), residence time and CO<sub>2</sub> loading (Figure 13b) are reported. Per segment, we calculate the initial dissolved oxygen content (Figure 13c), and then apply the DNM to calculate oxygen consumption and MEA consumption. The total residence time along the packing is 3.7 minutes, and the liquid hold-up is 21.7 m<sup>3</sup>. The MEA consumption added up to 155 g/tonCO<sub>2</sub>.

As per the ODIN results, the combination of high temperatures and low (lean-range) loadings lead to higher degradation. The lean loading is 0.2, and the rich loading is 0.51 mol/mol. The loading of 0.45 is achieved after 10m of packing – for this range, the kinetics are calculated based on the linear inter- and extrapolation between the 0.2 and 0.3 loading values. From 10m onwards, the 0.5 loading kinetic parameters are used.

These results suggest that limiting the absorber temperature could be very beneficial in controlling MEA degradation.

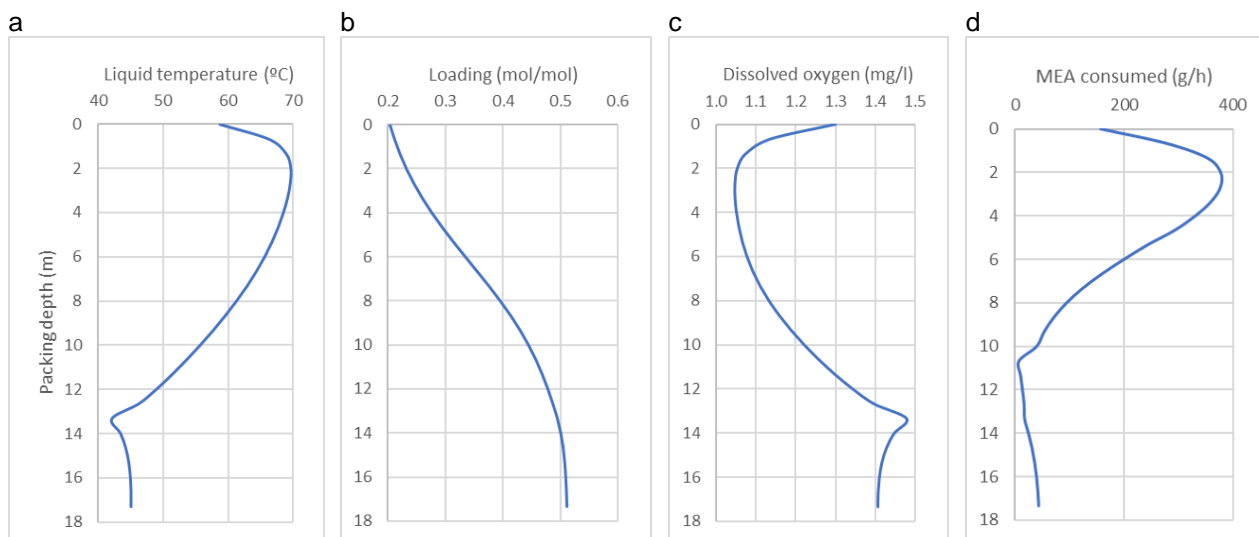


Figure 13. DNM applied to the absorber packing – MEA case

#### 4.2.3 Absorber packing – CESAR1

Applying the kinetic parameters and factor “a” values discussed, the CESAR1 consumption over the packing can be calculated, as given in Figure 14d.

The conceptual design considers an absorber packing height of 28m, with an intercooler at the lower packing section (21m packing depth). In the ProTreat simulation, the absorber packing is discretized into 31 segments, and for each segment a liquid temperature (Figure 14a), residence time and CO<sub>2</sub> loading (Figure 14b) are reported. Per segment, we calculate the initial dissolved oxygen content (Figure 14c), and then apply the DNM to calculate oxygen consumption and CESAR1 consumption. The total residence time along the packing is 5.4 minutes, and the liquid hold-up is 26.5 m<sup>3</sup>. The CESAR1 consumption added up to 15.8 g/tonCO<sub>2</sub>.

The model suggests that most of the CESAR1 consumption takes place in the bottom of the column, where loadings above 0.55 are achieved. This result may be misleading, as the kinetics parameters used for this range are extrapolations. For the loading range 0.1-0.4, the CESAR1 consumption is rather low in the absorber packing, despite the somewhat high temperatures achieved (up to 67°C).

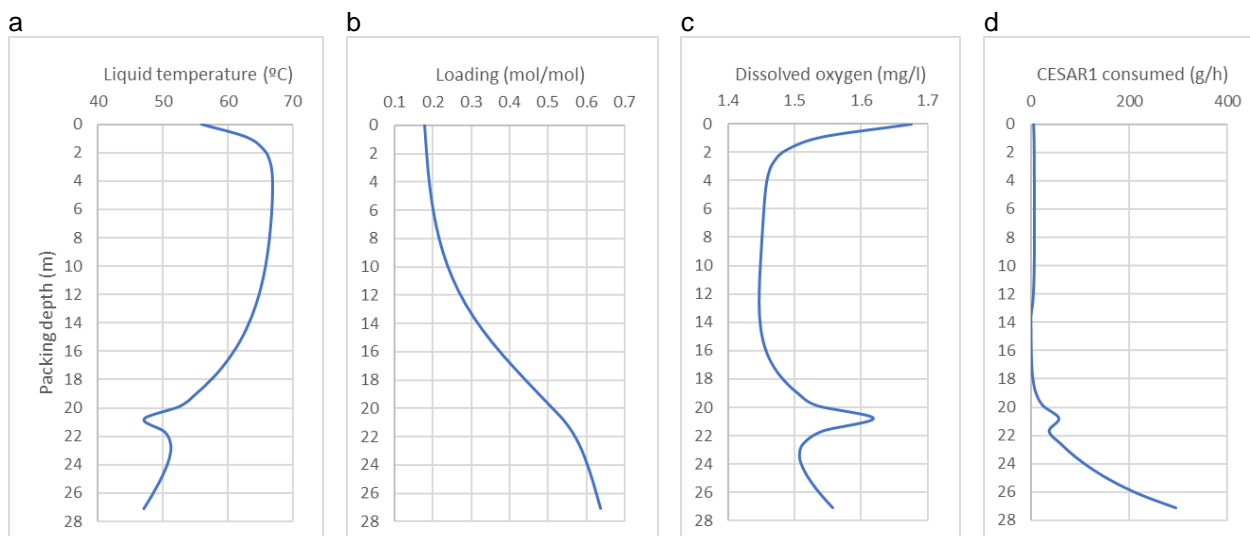


Figure 14. DNM applied to the absorber packing – CESAR1 case

#### 4.2.4 Absorber sump – MEA and CESAR1

The main parameters and calculated results are given in Table 8. As the kinetics of oxygen consumption in CESAR1 at rich loading is high (as a result of the proposed extrapolations), a higher solvent loss is calculated for CESAR1, as compared to MEA.

Table 8. Application of DNM at the absorber sump for MEA and CESAR1

Parameter	Unit	MEA	CESAR1
Residence time	min	6	6
Sump volume	m <sup>3</sup>	34.2	24.3
Rich loading	mol/mol	0.5	0.64
Temperature	°C	45.15	45.80
Initial DO	mol/l	$4.41 \cdot 10^{-5}$	$4.94 \cdot 10^{-5}$
Final DO	mol/l	$1.61 \cdot 10^{-5}$	$2.09 \cdot 10^{-6}$
Solvent consumed	g/h	855	3170
Solvent consumed	g/tonCO <sub>2</sub>	34.8	131

#### 4.2.5 Cross heat exchanger – MEA and CESAR1

In the cross heat exchanger, the rich solvent temperature is increased from ca. 45°C to ca. 100°C. However, the maximum temperatures in the ODIN tests were 50°C for MEA and 60°C for CESAR1. Therefore, we propose 2 scenarios for the cross heat exchanger. In the first (worst-case) scenario, we assume that all the dissolved oxygen that enters the heat exchanger is consumed. The ODIN data shows that the DO consumption is a strong function of temperature, and greatly accelerates between 20°C and 50-60°C for both solvents. On the other hand, in pilot operation with MEA, oxygen was detected as an impurity in the CO<sub>2</sub> product, indicating that the rich solvent that reaches the stripper still had some DO in it. In an alternative (best-case) scenario, the DNM is applied using low temperature kinetics. The design parameters and results are given in Table 9 and Table 10.

Table 9. Application of DNM at the cross heat exchanger for MEA and CESAR1: all DO is consumed

Parameter	Unit	MEA	CESAR1
Residence time	s	11.27	14.8
Cross HEX volume (rich side)	m <sup>3</sup>	1.1	1.0
Rich loading	mol/mol	0.5	0.64
Initial DO	mol/l	$1.61 \cdot 10^{-5}$	$2.09 \cdot 10^{-6}$
Final DO	mol/l	0	0
Solvent consumed	g/h	492	140
Solvent consumed	g/tonCO <sub>2</sub>	20	5.8

Table 10. Application of DNM at the cross heat exchanger for MEA and CESAR1: low T kinetics

Parameter	Unit	MEA	CESAR1
Residence time	s	11.3	14.8
Cross HEX volume (rich side)	m <sup>3</sup>	1.1	1.0
Rich loading	mol/mol	0.5	0.64
Initial DO	mol/l	$1.61 \cdot 10^{-5}$	$2.09 \cdot 10^{-6}$
Final DO	mol/l	$1.55 \cdot 10^{-5}$	$1.33 \cdot 10^{-6}$
Solvent consumed	g/h	20	35
Solvent consumed	g/tonCO <sub>2</sub>	0.8	1.5
O <sub>2</sub> in CO <sub>2</sub> product	ppmv	9.5	0.6

In the best case scenario only a fraction of the DO is consumed in the cross heat exchanger. Assuming that all DO leaving is unit would be stripped (i.e., neglecting further DO consumption in pipes and the stripper itself), the amount of oxygen in the CO<sub>2</sub> product is calculated.

#### 4.2.6 Consolidated results – MEA and CESAR1

The MEA and CESAR1 losses per equipment are given in Figure 15. This assumes the worst case scenario for the cross heat exchanger.

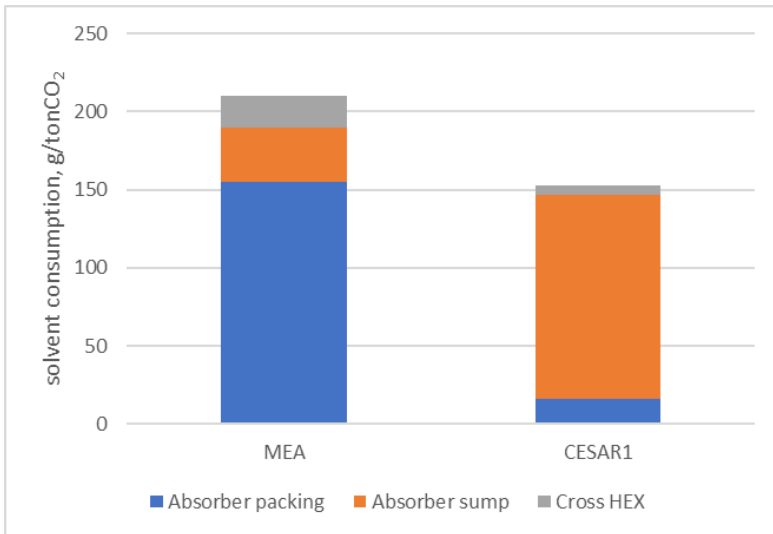


Figure 15. MEA and CESAR1 losses per equipment

## 5 Conclusions and future work

In this deliverable, the DNM is presented. The model can be applied to any solvent, regardless of the composition, as it relies solely on oxygen consumption data. The oxygen consumption data used in the current version of the DNM is generated with fresh solvent, in the absence of metals and degradation products. In order to obtain representative values, the stoichiometric factor is treated as a fitting parameter, and used to anchor the DNM results to those observed in the RWE pilot.

The DNM methodology is thoroughly discussed in the current deliverable, and the model can be used to predict solvent losses for MEA and CESAR1 at different operational conditions. This work is performed in WP6, where the degradation rate is calculated for full-scale coal- and gas-fired power plants, and the waste-to-energy case presented herein is revised. To improve the model prediction, more data is needed, as extensively discussed throughout this report.

Despite the DNM current limitations, general conclusions can already be taken. For MEA, it is likely that most of the solvent loss occurs already in the absorber packing (low loading, high temperature range). The absorber design could be modified in order to minimize losses – however, it should be taken into consideration that any changes would also affect the CO<sub>2</sub> absorption kinetics. So any proposed modification should be evaluated with a holistic view, considering CAPEX and OPEX impacts.

For CESAR1, most of the solvent degradation is expected to happen in the absorber sump. Lowering the residence time in the sump wouldn't necessarily lower the degradation, but is likely to just push it to the downstream unit operations. A possible solution would be to remove dissolved oxygen from the solvent before it enters the sump. Within LAUNCH, it was demonstrated that DORA is capable of removing at least 90% of DO from CESAR1 (see D2.1.2). Applying the DNM, it is estimated that DORA would lead to a reduction of ca. 80% in the CESAR1 loss (from 150 to 30 g/tonCO<sub>2</sub>).

## 6 References

- [1] S. A. Bedell, C. M. Worley, K. Darst, and K. Simmons, "Thermal and oxidative disproportionation in amine degradation-O<sub>2</sub> stoichiometry and mechanistic implications," *Int. J. Greenh. Gas Control*, vol. 5, no. 3, pp. 401–404, 2011, doi: 10.1016/j.ijggc.2010.03.005.
- [2] C. Gouedard, D. Picq, F. Launay, and P. L. Carrette, "Amine degradation in CO<sub>2</sub> capture. I. A review," *Int. J. Greenh. Gas Control*, vol. 10, pp. 244–270, 2012, doi: 10.1016/j.ijggc.2012.06.015.
- [3] T. Supap, R. Idem, P. Tontiwachwuthikul, and C. Saiwan, "Kinetics of sulfur dioxide- and oxygen-induced degradation of aqueous monoethanolamine solution during CO<sub>2</sub> absorption from power plant flue gas streams," *Int. J. Greenh. Gas Control*, vol. 3, no. 2, pp. 133–142, 2009, doi: 10.1016/j.ijggc.2008.06.009.
- [4] R. V. Figueiredo *et al.*, "Impact of dissolved oxygen removal on solvent degradation for post-combustion CO<sub>2</sub> capture," *Int. J. Greenh. Gas Control*, vol. 112, no. October, p. 103493, 2021, doi: 10.1016/j.ijggc.2021.103493.
- [5] D. D. D. Pinto, T. W. Brodtkorb, S. J. Vevelstad, H. Knuutila, and H. F. Svendsen, "Modeling of Oxidative MEA Degradation," *Energy Procedia*, vol. 63, pp. 940–950, 2014, doi: <https://doi.org/10.1016/j.egypro.2014.11.103>.
- [6] G. Léonard, D. Toye, and G. Heyen, "Experimental study and kinetic model of monoethanolamine oxidative and thermal degradation for post-combustion CO<sub>2</sub> capture," *Int. J. Greenh. Gas Control*, vol. 30, pp. 171–178, 2014, doi: <https://doi.org/10.1016/j.ijggc.2014.09.014>.
- [7] N. E. Flø *et al.*, "Results from MEA Degradation and Reclaiming Processes at the CO<sub>2</sub> Technology Centre Mongstad," *Energy Procedia*, vol. 114, no. November 2016, pp. 1307–1324, 2017, doi: 10.1016/j.egypro.2017.03.1899.
- [8] S. J. Vevelstad, M. T. Johansen, H. Knuutila, and H. F. Svendsen, "Extensive dataset for oxidative degradation of ethanolamine at 55–75°C and oxygen concentrations from 6 to 98%," *Int. J. Greenh. Gas Control*, vol. 50, pp. 158–178, 2016, doi: <https://doi.org/10.1016/j.ijggc.2016.04.013>.
- [9] AVR, "Sustainable Connection. Annual Report 2021," 2021. [Online]. Available: <https://avr.nl/wp-content/uploads/2022/04/AVR-Annual-Report-2021-Sustainable-connection.pdf>.